Appendix A. Supplementary data

A multifunctional sustainable ionohydrogel with excellent low-hysteresis driven mechanical performance, environmental tolerance, multimodal stimuli-responsiveness and power sources for wearable electronics

Wanjie Si,[ab] Yingpei Liang,[ab] Yukun Chen,[a] Shuidong Zhang*,[abc]

[a] College of Mechanical and Automotive, South China University of Technology, Guangzhou, 510640, China

[b] Guangdong Key Laboratory of Technique and Equipment for Macromolecular Advanced Manufacturing, South China University of Technology, Guangzhou, 510640, China

[c] State Key Laboratory of Pulp and Paper Engineering，South China University of Technology, Guangzhou, 510640, China

* Corresponding Author: Shuidong Zhang, Email: starch@scut.edu.cn

Table of Contents

Experimental Section

Materials. Regular corn starch consisting of 25 wt% amylose and 75 wt% amylopectin was purchased from Hengren Industry and Trade Co., Ltd. (China). Monomer acrylamide (AM) was obtained from Aladdin Co., Ltd. (Shanghai, China). N, N'-methylene bis(acrylamide) (MBA), Ammonium persulfate (APS, 99.99%) and borax ($Na_2B_4O_7 \cdot 10H_2O$) were acquired from Energy Chemical Co., Ltd. (China). Glycerol (AR, 99%) was supplied from Tianjin Damao Chemical Reagent Factory (China). Polydimethylsiloxane (PDMS) and commercial PVDF was purchased from the market. All chemicals were used directly without further purification. Deionized water was used for all experiments.

Preparation of starch/PAM/borax/glycerol (SPBG) ionohydrogel. The ionohydrogel was synthesized by the one-pot gelation-assisted polymerization method. The predesigned weight of dried starch was added into 40 ml, 0.1 M borax glycerol-aqueous solution (the volume ratio of glycerol/water=2:1) using mechanical stirring at 120 °C for 2h to form a homogeneous and viscous solution. To prevent vapor diffusion at high temperature, the beaker equipped with allihn type was sealed with silicone grease. Subsequently, AM (8 g) and MBA (80 mg) were added into the beaker and continuously stirred when the solution was cooled to freezing temperature. APS (60 mg) was quickly added under stirring after AM and MBA were completely dissolved in the solution. Then, the stirrer was constantly working under vacuum environment about 5 min to remove air bubbles. Finally, the uniform solution was gentle placed in PTFE mold, the ionohydrogel was obtained after polymerization process of AM at 65

°C for 6h. In this work, the polyacrylamide hydrogel was denoted as PAMH. The ionohydrogels with different compositions were coded as S_xP_yBG, where x and y represent the wt/mL of starch and AM to solvent volume. The ionohydrogels prepared by only changing borax concentrations and glycerol ratios were only named as the borax concentrations and the volume ratio of glycerol/water. The detailed compositions of ionohydrogels were shown in Table S1.

Fabrication of SPBG ionohydrogel strain sensor. The SPBG films were cut into rectangular strip to assemble resistance-type strain sensor. Copper wires as electrode were tightly linked to the end of the strip and the conductive silver paste was applied to make the interface compact between the electrode and the ionohydrogel.

Preparation of single-electrode SPBG ionohydrogel TENG. The single-electrode TNEG was prepared by SPBG, PDMS films and acrylic board with sandwiching structure, where SPBG, PDMS films and acrylic board served as the electrode layer, positive triboelectric layer and the support, respectively. Copper wires was contacted with SPBG for electrical signal output.

Characterizations.

The Fourier transform infrared (FTIR) spectrometer (Vector-33, Bruker, Germany), solid-state ^{13}C and ^{11}B nuclear magnetic resonance spectroscopy (NMR, Bruker 400 MHz, Germany), 1H-NMR spectra (Bruker 600 MHz, Germany) in DMSO-d_6, and X-ray photoelectron spectroscopy (XPS, ThermoScientific Escalab 250XI, USA) were conducted to analyze the chemical structure of SPBG ionohydrogel.

Anti-freezing and anti-drying property. The anti-freezing characterization of PAMH, SPG and SPBG were investigated using differential scanning calorimetry (DSC, METTLER, DSC 3), followed by equilibrated at -60 °C for 30 min, and heated to 200 °C at 10 °C/min rate under N_2 atmosphere. The anti-drying test of samples was measured by constant temperature and humidity test chamber (LS-TH-100S, China) at 25 °C and 50 %RH, respectively. The PAMH, SPG and SPBG ionohydrogels were made into a cylinder with a diameter of 20 mm and a height of 20 mm as original samples. At specific time intervals, the residual weight rate (RWR) was calculated with following formula:

$$RWR(\%) = \frac{w_r}{w_i} \times 100\% \qquad \text{(Equation S1)}$$

where w_r and w_i were the retention weight after losing water and initial weight of ionohydrogel, respectively.

Mechanical property. A universal tensile test was performed on testing platform (Wance 104B, China) equipped with 100 N force sensor to measure the mechanical performances. For the tensile test, five dumbbell shape specimens with a length of 75 mm and a width of 4 mm were conducted at 50 mm/min stretching rate. The cyclic compression tests were investigated using cylindrical ionohydrogel samples with a diameter of 20 mm and a height of 20 mm. Specially, to explore the anti-freezing property, the ionohydrogel were frozen at -20 and -40 °C for 4 hours before testing and carried out the test in the frozen environment.

Electrical measurement. The ionic conductivity of ionohydrogel was performed using electrochemical workstation (CHI 660E, China) on impedance spectrum in a frequency range of 10^{-2} to 10^6 Hz. The electrical property of SPBG sensors was measured with help of the universal testing machine and digital multimeter (DMM7510, Keithley, USA). For obtaining the real-time testing date, the and tensile signals were simultaneously recorded. Regarding to the measurement of human-related movement signals, the sensors were adhered on skin of the corresponding human parts and Cu electrodes were linked to DMM7510 for coinstantaneous detection. During the experiment, the sensors and the volunteer's skin were separated by the commercial polypropylene films to protect the volunteer. The electrical output performance of the single-electrode ionohydrogel based TNEG were recorded using electrochemical device (MT6514S, USA).

Table S1. The experimental ingredients and nomenclatures of the as-prepared hydrogel and ionohydrogels.

Samples	Starch (g)	Acrylamide (g)	Borax (M)	Glycerol (mL)	Water (mL)
PAMH	0	8	0	0	40
$S_{0.025}P_{0.2}BG$	1	8	0.1	26.7	13.3
$S_{0.075}P_{0.2}BG$	3	8	0.1	26.7	13.3
$S_{0.125}P_{0.2}BG$	5	8	0.1	26.7	13.3
$S_{0.175}P_{0.2}BG$	7	8	0.1	26.7	13.3
$S_{0.025}P_{0.2}H$	1	8	0	0	40
$S_{0.075}P_{0.2}H$	3	8	0	0	40
$S_{0.125}P_{0.2}H$	5	8	0	0	40
$S_{0.175}P_{0.2}H$	7	8	0	0	40
$S_{0.125}P_{0.2}G(1/5)$	5	8	0	6.7	33.3
$S_{0.125}P_{0.2}G(1/2)$	5	8	0	13.3	26.7
$S_{0.125}P_{0.2}G(1/1)$	5	8	0	20	20
$S_{0.125}P_{0.2}G(2/1)$	5	8	0	26.7	13.3
$S_{0.125}P_{0.2}BG$-0.02	5	8	0.02	26.7	13.3
$S_{0.125}P_{0.2}BG$-0.04	5	8	0.04	26.7	13.3
$S_{0.125}P_{0.2}BG$-0.06	5	8	0.06	26.7	13.3
$S_{0.125}P_{0.2}BG$-0.08	5	8	0.08	26.7	13.3

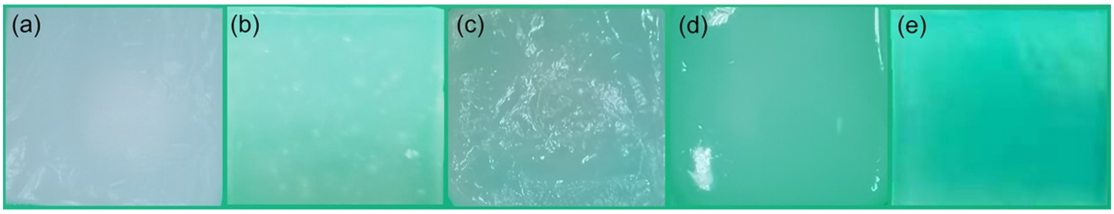

Fig. S1. Direct images of a) starch hydrogel, b) starch/glycerol gel, c) starch/borax hydrogel, d) starch/PAM hydrogel and e) starch/PAM/borax/glycerol ionohydrogel.

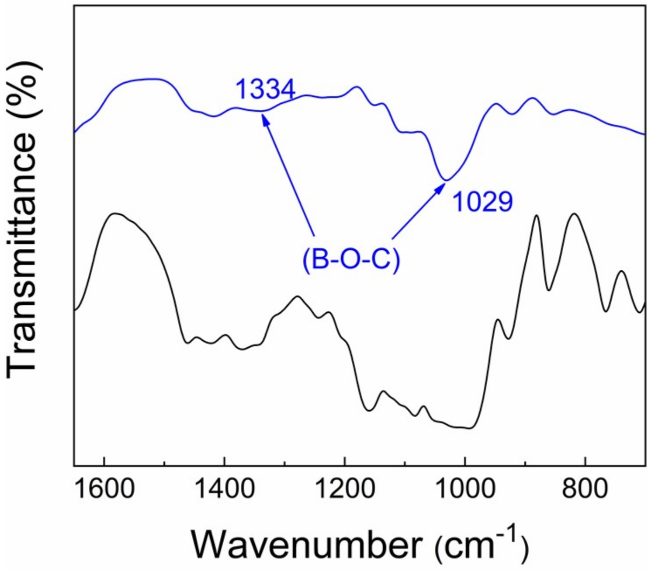

Fig. S2. Partially enlarged FTIR spectra of starch and SPBG ionohydrogel in the range of 1650-700 cm^{-1}.

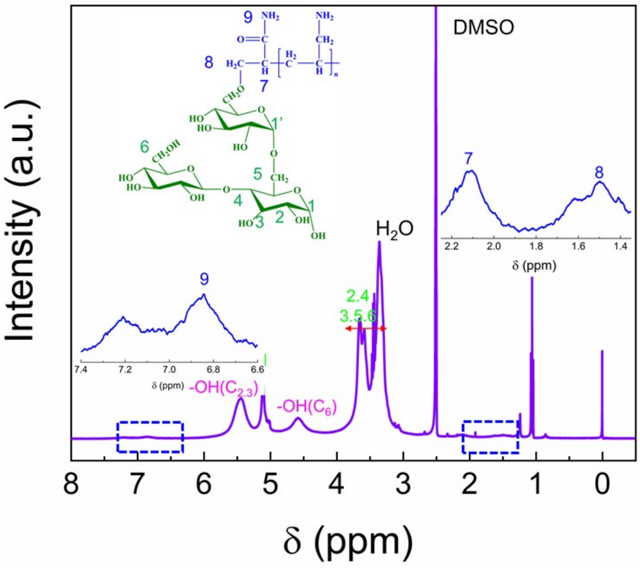

Fig. S3. ^{1}H-NMR spectra of starch-PAM in DMSO-d$_6$.

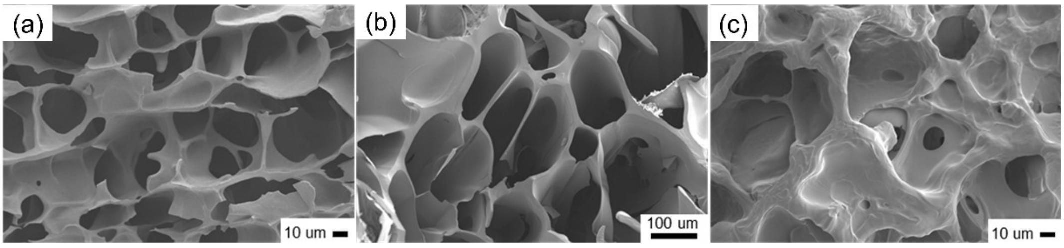

Fig. S4. SEM images of a) starch hydrogel, b) PAM hydrogel, and c) starch/PAM/borax hydrogel, respectively.

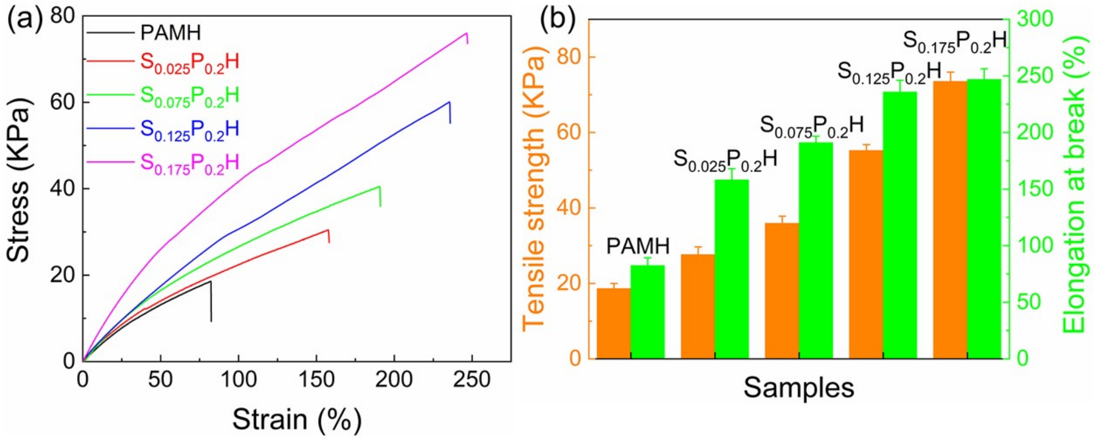

Fig. S5. a) Typical stress-strain curves and b) corresponding tensile strength and elongation at break values of SPHs with different starch contents.

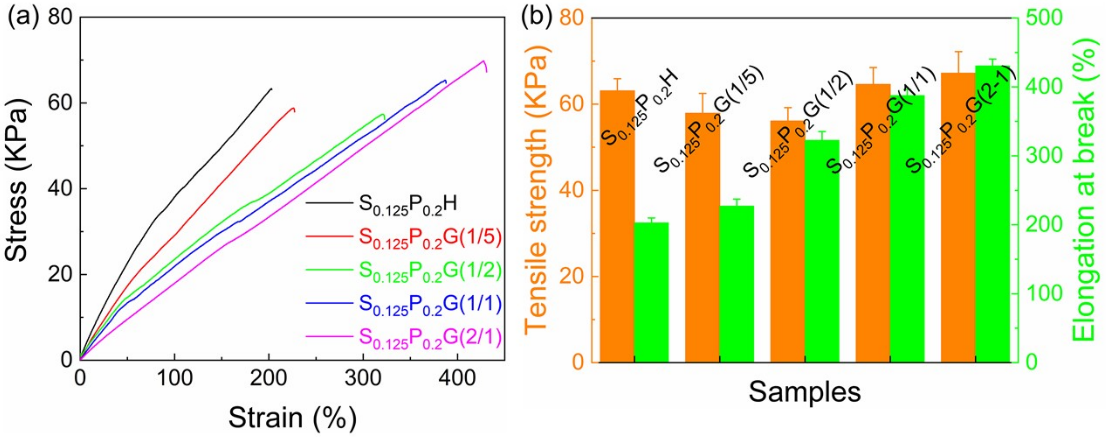

Fig. S6. a) Typical stress-strain curves and b) corresponding tensile strength and elongation at break values of SPGs with different glycerol/water volume ratio.

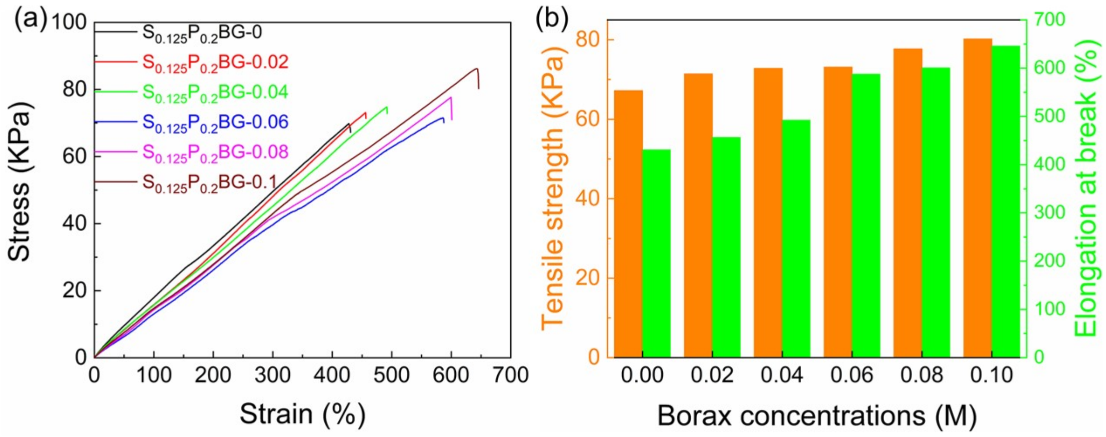

Fig. S7. a) Typical stress-strain curves and b) corresponding tensile strength and elongation at break values of SPBGs with different borax concentrations.

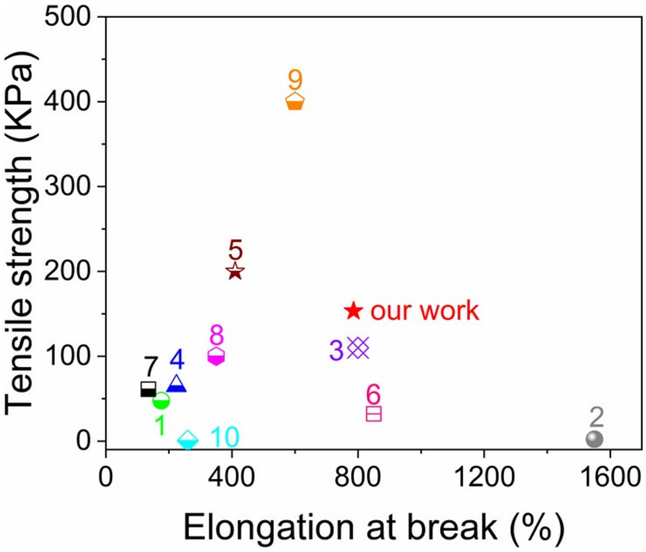

Fig. S8. The mechanical properties of reported conductive hydrogels for flexible electronic sensors.[1-10]

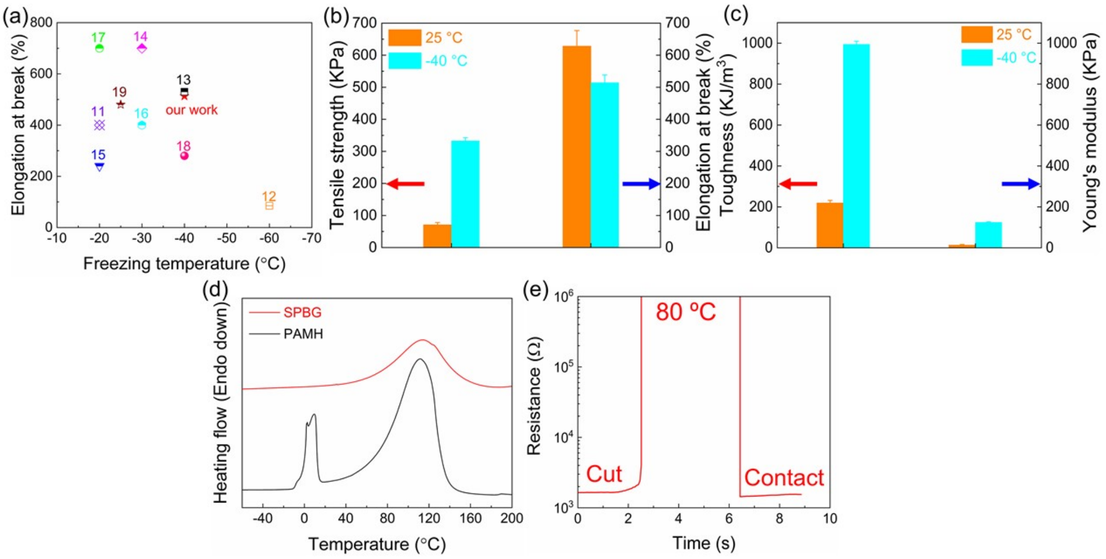

Figure S9. a) The stretching strain and freezing temperature of reported anti-freezing gel.[11-19] b) Tensile strength and elongation at break. c) Toughness and Young's modulus of SPBG ionohydrogel. d) DSC curves of PAMH and SPBG ionohydrogel. e) Resistance changes of SPBG in real time by cutting and contacting at 80 ºC.

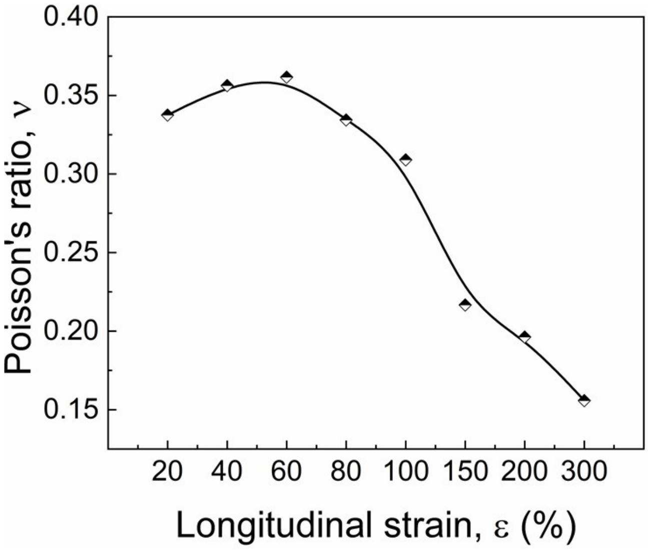

Figure S10. The Poission's ratio as function of longitudinal strain from 0 to 300%.

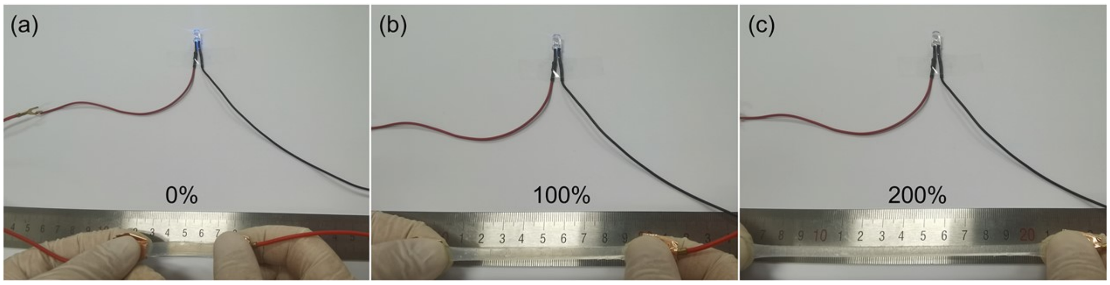

Figure S11. The brightness change images of LED are obtained during the process of stretching the SPBG ionohydrogel.

$$\rho = \frac{RS}{l} \qquad \text{(Equation S2)}$$

Where ρ is the volume resistivity, R, S and *l* is the volume resistivity, cross-sectional area and length. The Poisson's ratio is the absolute value of transverse and longitudinal strains. Therefore, the volume resistivity of the ionohydrogel can be formulated by:

$$\rho = \frac{R \times d}{\nu} \qquad \text{(Equation S3)}$$

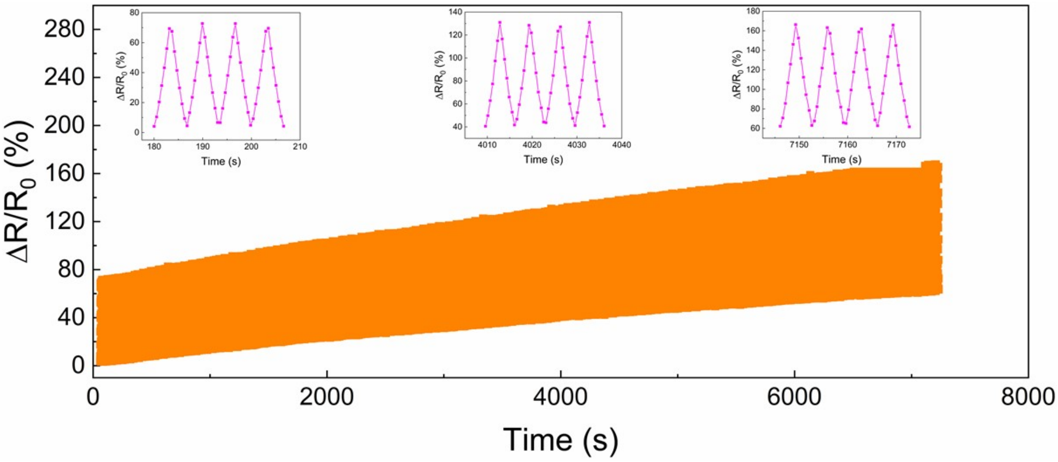

Figure S12. Resistance response of the sensor to applied tensile strain of 100% for 1000 cycles.

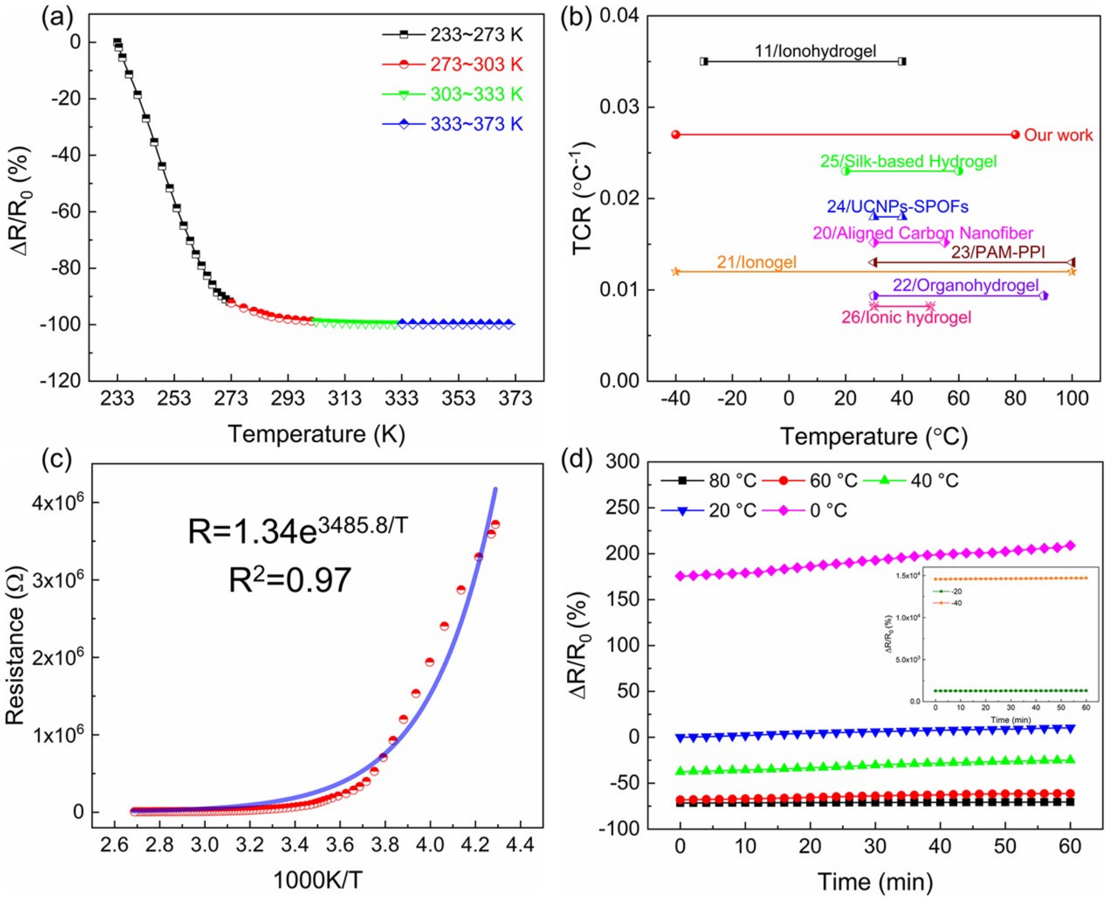

Fig. S13. a) Relative resistance variation with increasing temperature from 233 to 373K. b) Comparison of the temperature sensor in the present work with other representative flexible temperature sensors in terms of the working temperature range and temperature sensitivity.[11,20-26] c) The resistance of sensor versus temperature shows by Arrhenius law. d) The relative resistance of the ionohydrogel responds to external temperature from -40 to 80 °C for 1h.

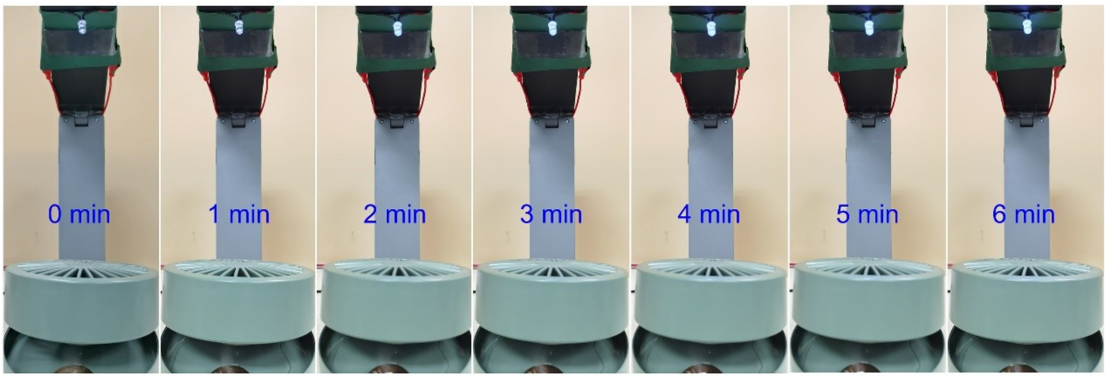

Fig. S14. The photographs of the brightness of an LED light at different times with humidification.

References

1 S. Zeng, J. Y. Zhang, G. Q. Zu and J. Huang, *Carbohyd. Polym.*, 2021, **267**, 118198 Contents

2 Y. L. Wang, H. L. Huang, J. L. Wu, L. Han, Z. L. Yang, Z. C. Jiang, R. Wang, Z. J. Huang and M. Xu, *ACS Sustain. Chem. Eng.*, 2020, **8**, 18506-18518.

3 X. D. Wang, Z. S. Wang, X. Y. Wang, L. Y. Shi and R. Ran, *Carbohyd. Polym.*, 2021, **257**.

4 R. Wang, M. J. Yao, S. Huang, J. L. Tian and Z. Q. Niu, *Adv. Funct. Mater.*, 2021, **31**.

5 J. C. Song, S. Chen, L. J. Sun, Y. F. Guo, L. Z. Zhang, S. L. Wang, H. X. Xuan, Q. B. Guan and Z. W. You, *Adv. Mater.*, 2020, **32**.

6 X. P. Morelle, W. R. Illeperuma, K. Tian, R. B. Bai, Z. G. Suo and J. J. Vlassak, *Adv. Mater.*, 2018, **30**.

7 Q. Z. Lin, H. Li, N. Ji, L. Dai, L. Xiong and Q. J. Sun, *Carbohyd. Polym.*, 2021, **251**.

8 J. Lai, H. Zhou, Z. Jin, S. Li, H. Liu, X. Jin, C. Luo, A. Ma and W. Chen, *ACS Appl. Mater. Inter.*, 2019, **11**, 26412-26420.

9 X. Jing, H. Y. Mi, X. F. Peng and L. S. Turng, *Carbon*, 2018, **136**, 63-72.

10 J. Hou, M. S. Liu, H. C. Zhang, Y. L. Song, X. C. Jiang, A. B. Yu, L. Jiang and B. Su, *J. Mater. Chem. A*, 2017, **5**, 13138-13144.

11 X. R. Zhang, C. Cui, S. Chen, L. Meng, H. N. Zhao, F. Xu and J. Yang, *Chem. Mater.*, 2022, **34**, 1065-1077.

12 X. F. Zhang, X. F. Ma, T. Hou, K. C. Guo, J. Y. Yin, Z. G. Wang, L. Shu, M. He and J. F. Yao, *Angew Chem Int Edit*, 2019, **58**, 7366-7370.

13 Q. Y. Yu, Z. H. Qin, F. Ji, S. Chen, S. Y. Luo, M. M. Yao, X. J. Wu, W. W. Liu, X. Sun, H. T. Zhang, Y. L. Zhao, F. L. Yao and J. J. Li, *Chem. Eng. J.*, 2021, **404**.

14 Z. Y. Xu, F. H. Zhou, H. Z. Yan, G. R. Gao, H. J. Li, R. Li and T. Chen, *Nano Energy*, 2021, **90**.

15 M. Wu, X. Wang, Y. Xia, Y. Zhu, S. Zhu, C. Jia, W. Guo, Q. Li and Z. Yan, *Nano Energy*, 2022, **95**, 106967.

16 Z. H. Qin, X. Sun, H. T. Zhang, Q. Y. Yu, X. Y. Wang, S. S. He, F. L. Yao and J. J. Li, *J. Mater. Chem. A*, 2020, **8**, 4447-4456.

17 J. Lu, J. F. Gu, O. D. Hu, Y. H. Fu, D. Z. Ye, X. Zhang, Y. Zheng, L. X. Hou, H. Y. Liu and X. C. Jiang, *J. Mater. Chem. A*, 2021, **9**, 18406-18420.

18 J. Lan, Y. S. Li, B. Yan, C. X. Yin, R. Ran and L. Y. Shi, *ACS Appl. Mater. Inter.*, 2020, **12**, 37597-37606.

19 G. Ge, W. Yuan, W. Zhao, Y. Lu, Y. Z. Zhang, W. J. Wang, P. Chen, W. Huang, W. L. Si and X. C. Dong, *J. Mater. Chem. A*, 2019, **7**, 5949-5956.

20 J. H. Lee, H. M. Chen, E. Kim, H. Zhang, K. Wu, H. M. Zhang, X. Shen, Q. B. Zheng, J. L. Yang, S. Jeon and J. K. Kim, *Mater. Horiz.*, 2021, **8**, 1488-1498.

21 N. Jiang, X. H. Chang, D. W. Hu, L. R. Chen, Y. P. Wang, J. W. Chen and Y. T. Zhu, *Chem. Eng. J.*, 2021, **424**.

22 J. F. Gu, J. R. Huang, G. Q. Chen, L. X. Hou, J. Zhang, X. Zhang, X. X. Yang, L. H. Guan, X. C. Jiang and H. Y. Liu, *ACS Appl. Mater. Inter.*, 2020, **12**, 40815-40827.

23 H. T. Yu, Y. T. Guo, C. Yao, D. F. Perepichka and H. Meng, *J. Mater. Chem. C*, 2016, **4**, 11055-11058.

24 J. J. Guo, B. Q. Zhou, C. X. Yang, Q. H. Dai and L. J. Kong, *Adv. Funct. Mater.*, 2019, **29**.

25 Y. Hu, M. Zhang, C. R. Qin, X. Y. Qian, L. N. Zhang, J. P. Zhou and A. Lu, *Carbohyd. Polym.*, 2021, **265**.

26 S. J. Feng, Q. R. Li, S. X. Wang, B. Wang, Y. T. Hou and T. Zhang, *ACS Appl. Mater. Inter.*, 2019, **11**, 21049-21057.